

# Influence of static and dynamical structural changes on ultrafast processes mediated by conical intersections

J. Voll, T. Kerscher, D. Geppert, R. de Vivie-Riedle\*

LMU Department Chemie, Butenandt-Str. 11, 81377 München, Germany

Available online 3 February 2007

## Abstract

The technological needs imposed by the exponential miniaturization trend of conventional electronic devices has drawn attention towards the development of smaller and faster devices like ultrafast molecular switches. In recent years molecular switches emerge again in the focus of active and innovative research with state-of-the-art optical tools recording their dynamics in real time. Still many questions about the underlying microscopic mechanism are left open, including potential factors that effect the switching process in either way, improve or worsen it. Due to the complexity of such molecules it is difficult to obtain a global answer from experiment alone. On the other side molecular switches are generally too large for a complete quantum chemical and quantum dynamical calculation. In our group we therefore developed an ab initio based modular model to handle the laser induced quantum dynamics in molecular switches like fulgides. It enables us to study the effect of internal molecular coupling and of the molecular response to external fields. We can investigate the related wave packet dynamics, the switching efficiency and the controllability. Our results focus on the laser induced ring opening in fulgides, which equals one direction of the switching process. Presented are the influence of a conical intersection seam and of time-dependent potentials, mimicking the mean interaction with the environment. Furthermore the relation of controllability and the wave packet's momentum is studied and the influence of potential barriers on the switching dynamics is shown.

© 2007 Elsevier B.V. All rights reserved.

**Keywords:** Molecular photo switches; Photogromic fulgides; Ultrafast quantum dynamics; Extended conical intersections; Time-varying potentials; Control concepts

## 1. Introduction

Photochromism is a prominent feature of fulgides and their derivatives which are therefore studied and discussed as potential molecular switches. Several other systems like diarylethenes, azobenzene or rotaxanes are also promising candidates. A comprehensive overview of possible molecular systems and their fields of application is given in Ref. [1]. A *cis-trans* isomerization as switching mechanism is often found in nature, e.g. in retinal it plays the crucial role in the vision process. This isomerization is studied from many viewpoints, including also the quantum dynamical and control aspects [2–6].

In our work we concentrate on the photo switching of fulgides. Its two isomers C and E can be transferred into each

other by light irradiation (Fig. 1). Beyond their possible application as memory storage device they can selectively enable or disable energy or electron transfer processes between a donor and an acceptor molecule [7,8]. Experiments show that the switching process in both directions, ring closure as well as ring opening, occur ultrafast in the femto- to picosecond regime [7,9,10]. Light absorption and rearrangement of the molecular frame are predominantly restricted to the active center, thus the discussion of the microscopic mechanism can be concentrated on the switching process of the chromophoric center cyclohexadiene/hexatriene (Fig. 1). After light excitation to a higher electronic state the system returns through multiple conical intersections (CoIn) back to the electronic ground state where the reaction pathway bifurcates towards the desired product and back to the educt. For an optimal molecular switch the final product distribution should be accumulated in the wanted isomer. Experimental works, however, show that only a minor product yield is obtained by laser irradiation [11]. Optimization of the switching process can be obtained in quantum dynamical calculations by using modulated femtosecond laser fields [12,13]. Furthermore

\* Corresponding author. Tel.: +49 89 218077533.

E-mail addresses: [Judith.Voll@cup.uni-muenchen.de](mailto:Judith.Voll@cup.uni-muenchen.de) (J. Voll),  
[Tobias.Kerscher@cup.uni-muenchen.de](mailto:Tobias.Kerscher@cup.uni-muenchen.de) (T. Kerscher),  
[Dorothee.Geppert@cup.uni-muenchen.de](mailto:Dorothee.Geppert@cup.uni-muenchen.de) (D. Geppert),  
[Regina.de\\_Vivie@cup.uni-muenchen.de](mailto:Regina.de_Vivie@cup.uni-muenchen.de) (R. de Vivie-Riedle).

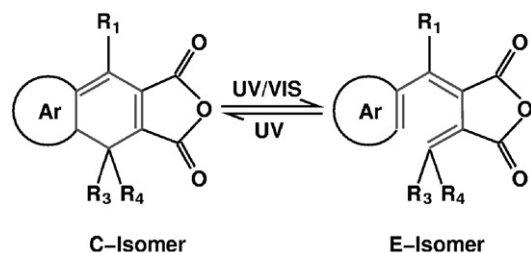


Fig. 1. Switching process of fulgides with aromatic (Ar) and aliphatic ( $R_i$ ) substituents.

modifications of the molecular system can induce both static and dynamic changes to the electronic potential energy surfaces (PES) and to the coupling between them. These modifications can be caused by solvent and environmental effects or achieved by an exchange of heteroatoms or substituents.

The development of a modular model based on the energetics and dynamics of the chromophoric center in fulgides allows us to investigate how such modifications may influence the dynamics and the switching efficiency. In detail we will present the effect of a seam of CoIns on the dynamics followed by a demonstration of using the momentum of the excited wave packet to control the product yield. We show which effect time-dependent varying PES, simulating the interaction with the environment, may have on the quantum dynamics. Finally the influence that barriers on the excited states may have on the switching process is studied.

## 2. The model system

In our investigations we solve the time-dependent Schrödinger equation for the nuclear motion in the matrix representation (Eq. (1)):

$$i \frac{\partial}{\partial t} \psi(t) = \left\{ \begin{pmatrix} T_{\text{nuc}} & K_{12} \\ -K_{12} & T_{\text{nuc}} \end{pmatrix} + \begin{pmatrix} V_1 & -\mu_{12} \in(t) \\ -\mu_{12} \in(t) & V_2 \end{pmatrix} \right\} \times \begin{pmatrix} \psi_1(t) \\ \psi_2(t) \end{pmatrix}. \quad (1)$$

In case of the chromophore both PES ( $V_1 = S_0$  and  $V_2 = S_1$ ), the non-adiabatic coupling elements ( $K_{12}$ ) and the dipole moment ( $\mu_{12}$ ) are based on quantum chemical ab initio calculations on CASSCF or CASPT2 level [12,14–18]. The fulgide model is set up by analytical functions adapted to these quantum chemical and additional quantum dynamical results of the chromophore. The resulting PES in Fig. 2 are spanned by the reactive coordinates  $r$  and  $\varphi$  of the active center. The reactive coordinates have been deduced in Ref. [17] and describe all important structural changes occurring on the femtosecond time scale. They consist of up to 15 normal modes [19], thus the resulting PES specify a curvilinear reaction space including the minimum energy path of the switching process. As in these calculations the remaining vibrational degrees are relaxed, their contribution to the reaction is included in the PES in form of a static meanfield. All simulations in this work refer to the specific compound furyl fulgide (Fig. 3).

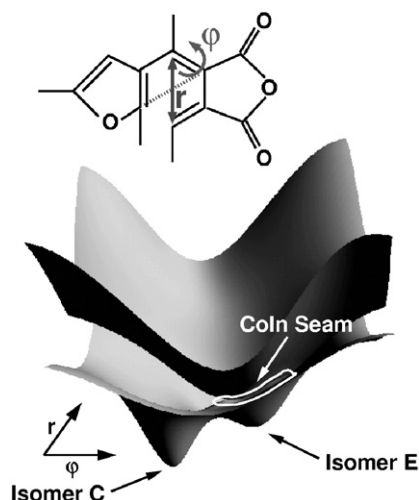


Fig. 2. Reactive coordinates  $r$  and  $\varphi$  of the chromophore (top).  $r$  describes an asymmetric squeezing and  $\varphi$  is the angle between the two indicated diagonals. The resulting PES are shown below.

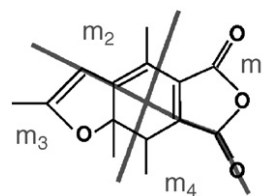


Fig. 3. Partitioning of furyl fulgide into four mass points. The atoms on the lines are splitted up between the corresponding mass points.

The kinetic part  $T_{\text{nuc}}$  of the corresponding Hamiltonian was constructed according to the reactive coordinates [17]:

$$T_{\text{nuc}} = -\frac{1}{2} \left\{ \frac{B}{r} \frac{\partial^2}{\partial r^2} r + \left( \frac{B}{r^2} + \frac{\tilde{B}}{\tilde{r}^2} \right) \frac{1}{\sin^2 \vartheta_0} \frac{\partial^2}{\partial \varphi^2} \right\}. \quad (2)$$

Here  $B$  and  $\tilde{B}$  are the inverse reduced masses  $B = (1/m_2) + (1/m_4)$  and  $\tilde{B} = (1/m_1) + (1/m_3)$ . The compound is separated into four parts, like depicted in Fig. 3 and the resulting masses (given in a.u.) are  $m_1 = 138,596$ ,  $m_2 = 72,123$ ,  $m_3 = 150,600$  and  $m_4 = 113,203$ . The angle  $\vartheta_0$  describes the planar ring opening and can be set to the fixed value of 1.0105 rad [17].

The modular set up enables us to adapt the PES to experimental and ongoing theoretical observations. Possible scenarios can be tested and their consequences on the dynamics, the product ratio and the resulting control possibilities can be predicted. In the following we present selected molecular modifications and environmental influences concerning the ring opening reaction, i.e. the switching from isomer C to isomer E.

## 3. Conical intersection seam

Conical intersections in chemical systems, earlier seen as rarity, are nowadays regarded as important components of ultrafast photochemical and biological reactions. The dimension of the conical intersection space scales with the internal vibrational degrees of freedom. Considering systems with many atoms it

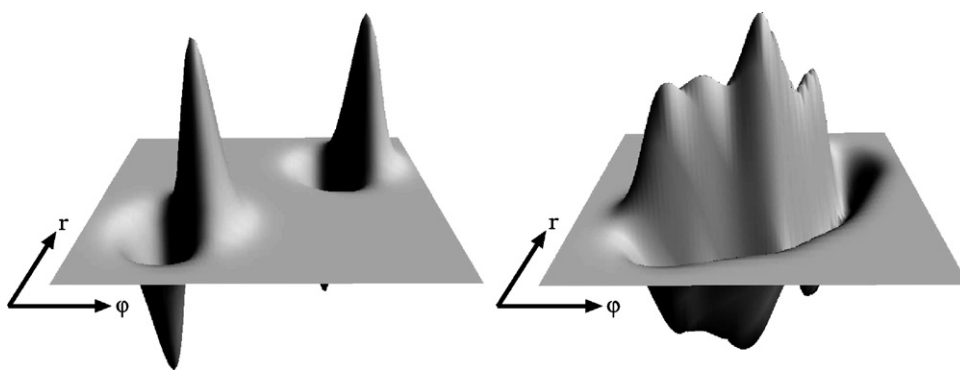


Fig. 4. Non-adiabatic coupling elements. Two separated CoIns (left) and the extrapolated seam of CoIns (right).

is conceivable that not only one or two CoIns are energetically reachable, but a whole seam of them. In the recent years quantum chemical methods were developed to localize such seams [20,21]. A conical intersection seam was reported in the literature for cyclohexadiene [22]. It connects the energetically lowest CoIn in  $C_2$ -symmetry with the CoIn of global minimal energy following the gradient in the space of CoIns. We assume a similar feature in the larger fulgides.

As outlined in Section 2 our reactive mode ansatz differs from the typical normal mode ansatz as each reactive coordinate is a linear combination of several normal modes with spatially dependent coefficients. The flexibility of these reactive coordinates, together with the adiabatic description, makes it possible to incorporate the conical intersection seam in the form of a projection into this subspace. Fig. 4 depicts the different non-adiabatic coupling elements used in our model system. The left picture shows two separated coupling elements, their integral and position are adjusted to the ab initio data of cyclohexadiene [18]. The CoIn at larger  $r$  and  $\varphi$  values corresponds to higher potential energy and is called CoIn-2 throughout this paper, the other CoIn (CoIn-1) lies in the vicinity of the excited state minimum. The coupling elements in case of the seam (right picture) were constructed adding further coupling elements of the same size and shape between CoIn-1 and CoIn-2. Additionally the PES were readjusted in the coupling region to become energetically degenerated.

Comparing the dynamics of the model system containing two CoIns and the seam, respectively, reveals an intensified coupling between the PES, but no essential differences in the wave packet motion. For a period of 300 fs the transfer efficiency is enhanced from 40 to 60%. After laser excitation the wave packet oscillates between the Franck–Condon and the coupling region defined by the conical intersection seam. Each time it reaches the coupling region population is transferred from the excited to the ground state which results in a step-wise increase of the ground state population (Fig. 5). The height of the steps decreases in time, due to the diminishing excited state population and the spreading of the wave packet. A prominent feature is that the excited wave packet dynamics changes in the first two oscillation periods from a clockwise to a counter clockwise motion along the coupling seam. Back on the ground state, the  $S_0$  wave packet carries high momentum. Parts of the wave packet are damped

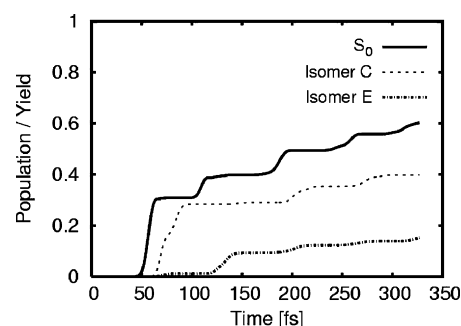


Fig. 5.  $S_0$  population and product yields of a wave packet propagation with the CoIn seam after excitation with a Gaussian shaped laser pulse ( $\omega_0 = 233$  nm, FWHM = 11 fs).

away at the actual grid boundaries to avoid numerical errors due to the periodic boundary condition. This leads to losses of the overall quantum yield but it also avoids the unphysical return to the excited state via the CoIns in large molecular systems. To obtain the product yields for the single isomers a local projection of the ground state wave packet on both minima is performed.

Analyzing the corresponding ground state dynamics one observes a continuation of the propagating direction in the excited state dynamics: after the first coupling step (clockwise motion) the educt is formed while the second coupling step (counter clockwise motion) primarily leads to the desired isomer E (Fig. 5). The enhancement of the coupling to the ground state by the seam dominantly occurs during the first coupling step and can be assigned to the expanded region of effective coupling elements. Due to the dynamics of the wave packet the dominant coupling region is still localized at the energetically higher CoIn-2, like it was observed in earlier calculations of the isolated chromophore [12,18] and for the fulgide model [23].

#### 4. Controlled pathways through the conical intersection seam

The dynamics of a suitable molecular switch must be controllable to guarantee an entire transformation between the two isomers. In earlier publications we presented our ansatz to control the ring *closure* reaction using shaped femtosecond laser

pulses: the laser pulse induces a wave packet on the excited state with initial components of momentum leading it to the desired target. The required shape of the laser is determined by optimal control theory [24–28]. Two different control concepts were proposed and realized which can handle the system's specific limitation, namely the restriction of the transition dipole moment to the Franck–Condon regions of both isomers [12,13]. Thereby the control is complicated as the conical intersections lie in the optically dark region.

Within the scope of our model the control of the ring *opening* reaction with optimally shaped UV pulses is not possible as additional challenges occur. Due to the topology of the excited state surface in the Franck–Condon region of isomer C the laser excited wave packet gains a huge momentum in  $\varphi$  direction and almost none in  $r$ . This results in a certain controllability in  $\varphi$ , whereas the momentum in  $r$  cannot be influenced. In earlier publications [12] we noticed that the momentum of the wave packet on the excited state while passing the CoIns effects the ground state dynamics and thereby the product distribution. To obtain control of the reaction outcome, we combine this fact with our experience from the dynamics in the presence of the CoIn seam (Section 3). This means a wavepacket is needed in the excited state which approaches the efficient coupling region in a counter clockwise manner. As the momentum in  $r$  cannot be controlled directly by UV-excitation, one could resort to previous femtosecond IR-excitation that prepares a ground state wave packet oscillating in  $r$  direction as demonstrated by the group of Manz and co-workers [29]. We simulated such a scenario by placing a ground state wave packet at different positions on the S-1 state in the optically reachable region of the closed isomer C.

As expected, the dynamics on the excited state changes and an intense influence on the coupling effectiveness as well as on the product distribution is noticed. From the temporal evolution of the spatial expectation values of the  $S_1$  wave packet we obtained a trajectory for each initial position. The two most remarkable results for the first few femtoseconds are shown in Fig. 6. Due to the shape of the excited PES (solid black contour lines) a displacement of the wave packet can result in a reversed direction (clockwise to counter clockwise) while passing the

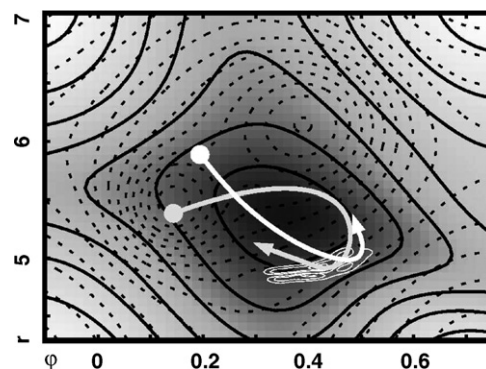


Fig. 6. Temporal evolution of the spatial expectation value of two initial wave packets on  $S_1$  (solid black contour, units in a.u.) which have been displaced from the Franck–Condon region. Additionally  $S_0$  (dashed contour) and the non-adiabatic coupling elements (solid white contour) are shown.

coupling region (shown in Fig. 6). For an effective switching process the mechanism has to comply with two conditions: the first is a complete population transfer back to the ground state and the second is the exclusive formation of the target isomer. To enlighten the mechanism, we compare the time-dependent  $S_0$  population of the two displaced initial wave packets (Fig. 7) with the primary one induced by UV excitation (Section 3, Fig. 5).

A large gain in coupling efficiency is recognized with a displacement to smaller  $r$ -values (Fig. 7, left). This increase in coupling efficiency arises because the wave packet fully reaches the coupling region and follows the seam for a short period. In case of the selected displacement to larger  $r$ -values a decrease of coupling efficiency is observed as now only parts of the wave packet reach the coupling region. Comparing their product yields, after the first coupling step there is an obvious change in product distribution. While a displacement to small  $r$ -values results in an enlarged back reaction to isomer C, a displacement to larger  $r$ -values favors the formation of the open isomer E. These findings confirm that during the coupling to the ground state the momentum of the wave packet is conserved and determines the dynamics on  $S_0$ . These facts can be used to control the ring opening reaction where a more targeted proceeding is still demanded.

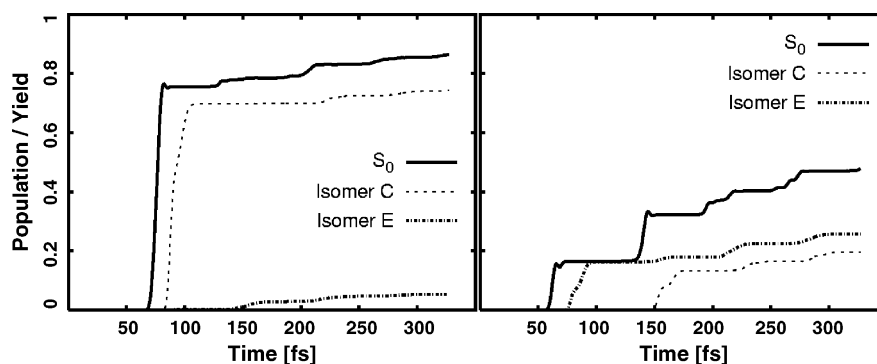


Fig. 7.  $S_0$  population and product yields of the two propagations of, from the Franck–Condon region at  $(r_{FC}, \varphi_{FC}) = (5.48, 0.14)$ , displaced initial wave packets according to Fig. 6. Displacement to small values of  $r$  (initial state:  $(r_1, \varphi_1) = (5.38, 0.14)$ ) leads to an enlarged coupling and formation of isomer C (left). Displacement to large values of  $r$  (initial state:  $(r_2, \varphi_2) = (5.88, 0.19)$ ) promotes the formation of isomer E (right).

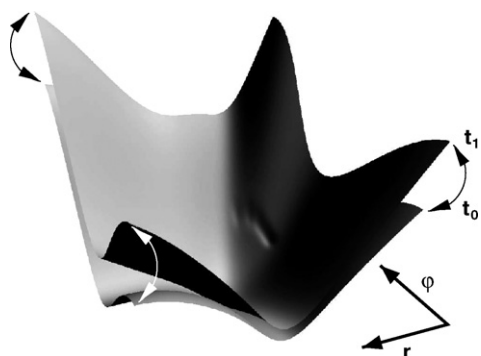


Fig. 8. Time-dependent PES. Shown is the shifted  $S_1$  state for the two extreme values for  $c(t)$ , the time-dependent sinusoidally varying penalty factor for the perturbation. To ensure excitation by the laser pulse, starting without perturbation:  $c(t_0) = 0$  (lower PES), and reaching maximum perturbation:  $c(t_1) = 1$  (higher PES) in arbitrary periods.

## 5. Time-dependent potentials

Environmental effects, e.g. solvent interaction, can influence the molecular dynamics. Slowdown of photochemical processes and change of excited state life times are reported for experiments with fulgide systems [11]. Besides a static influence the perturbation can have dynamical character. For example collisions with solvent molecules or just the change of the surrounding structure can alter the meanfield experienced by the considered system. A detailed analysis of the environment dynamics would require to average over several wave packet simulations varying the time-dependent perturbation as demonstrated for the *cis-trans* isomerization in retinal [2,4,5].

To evaluate the relevant time scales and the qualitative tendencies of the systems dynamical response to the environmental fluctuations, we introduce in a first step time-dependent perturbation to the PES (Fig. 8). During the propagation in the excited state, at each time step  $t$  an additional surface  $V_{\text{add}}$  was added with a time-dependent factor  $c(t)$  to the static PES  $S_i^0$ :  $S_i(t) = S_i^0 + c(t)V_{\text{add}}$ . The factor  $c(t)$  oscillates sinusoidally between 0 and 1 with different frequencies to cover different time scales. With increasing potential energy, i.e. in the region of highly excited vibrations, the density of states as well as the molecule's sensitivity to collisions rise. For this reason the additional potential  $V_{\text{add}}$  was chosen harmonic with its minimum at the minimum of the excited state  $S_1^0$ . Both surfaces vary in the same way, which

guarantees that the relative position of the CoIn seam is not affected by the solvent, as required from the similar character of the electronic states. To stay within the perturbative regime, the maximum additive energy was set to a 10th of the  $S_1^0$  potential difference the molecule experiences.

In Fig. 9 the resulting  $S_0$  population for two time varying potentials with different periods of 17 fs (left) and 0.4 ps (right) are shown exemplarily. In the following comparison with the static PES (Section 3, Fig. 5) we focus on the first coupling step, because this is the one that can be controlled. Only the fast oscillating perturbation (Fig. 9, left) effects the dynamics significantly. The coupling efficiency is enhanced simultaneously favoring isomer C. When the frequency is decelerated towards the picosecond regime, reflecting the movement of the surrounding solvent, the coupling efficiency is not enlarged. On a longer time scale an equal distribution of the both isomers is found (Fig. 9, right). From our results we can conclude that the controllability is not affected by environmental effects occurring on the picosecond and longer time scales.

## 6. Barriers along the reaction path

In the context of experimental observations the occurrence of several relaxation times is often explained by barriers on the excited PES. There are many reasons for the appearance of such barriers, e.g. steric effects which hinder the molecular flexibility, static environmental effects or electronic effects like the interaction with higher electronic PES. Ab initio calculations for the thienyl fulgide are performed on the CASSCF level using a 6-31G\* basis set and a (8, 8) complete active space. By geometry optimization of the  $S_1$  state at least two minima could be localized [23]. The details of the quantum chemical calculations will be published elsewhere together with the results of the ongoing work involving the relevant exciting states. The lower minimum is located between both isomers exhibiting a geometry of the central  $C_6$ -ring at that resembles the excited state minimum geometry of the isolated chromophore cyclohexadiene. The second minimum is located near the Franck–Condon region of the closed isomer C. The existence of two minima leads to a barrier between them, which is located close to the region where the initial wave packet is prepared by the laser excitation.

The effect of barriers different in shape, size and location was tested in the model system. In general they slow down the

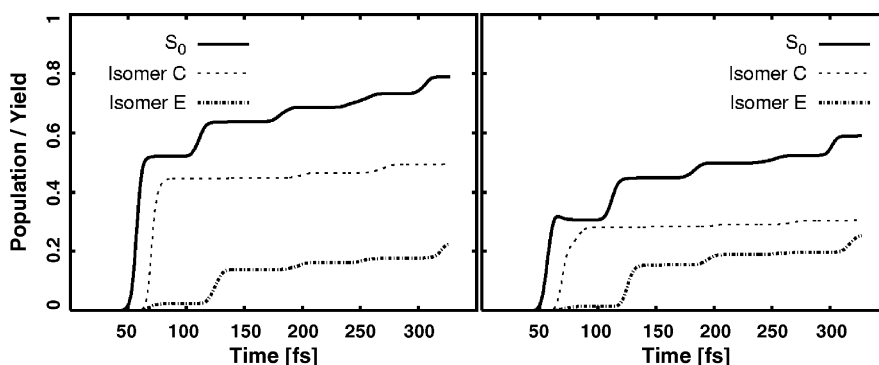


Fig. 9.  $S_0$  population and product yields of wave packet propagations with time-dependent PES varying with a period of 17 fs (left) and 0.4 ps (right).

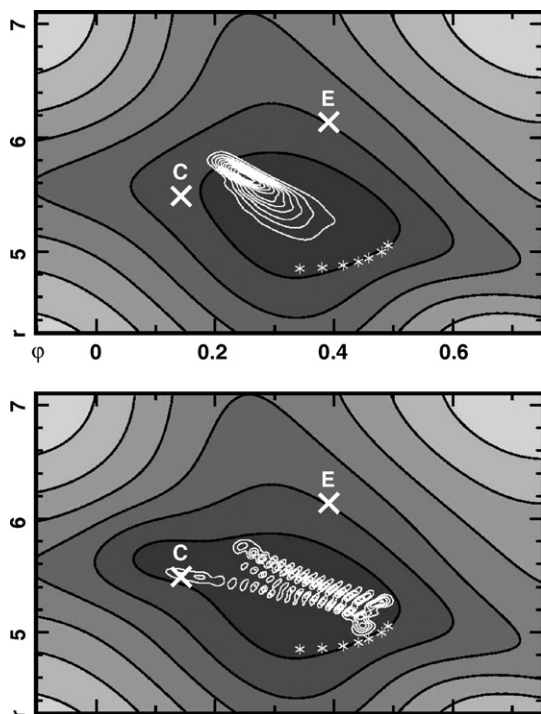


Fig. 10. Snapshots of wave packets at 70 fs after laser excitation on the  $S_1$  PES (a.u.), without barrier (top) and including a barrier close to the Franck–Condon region (bottom). Franck–Condon regions of isomer C and E are marked in white. The conical intersection seam is marked by white asterisks.

reaction velocity and induce interference effects. Especially barriers located in regions, where the wave packet has only little kinetic energy, seriously influence the dynamics. The slight minimum plus the barrier near the Franck–Condon region results in multiple effects. The gradient in the  $\varphi$  coordinate is reduced, therefore parts of the wave packet remain in the Franck–Condon region about four times longer than in case of the barrierless potential. This delayed propagation causes a wide spreading of the wave packet while moving towards the coupling region. After reflection at the turning point close to the effective coupling region (around CoIn-2), the faster components of the elongated wave packet interfere with the delayed ones. This leads to a nodal structure of the wave packet which already appears after a propagation time of 70 fs (Fig. 10, bottom). Once the nodal structure is formed, the wave packet does not refocus again during the switching process. In contrast, the wave packet, oscillating in the barrierless potential, stays localized during the whole propagation (Fig. 10, top). In consequence of the wave packet's spreading the coupling efficiency through the CoIn seam is lowered and the product yield is evenly distributed.

## 7. Conclusion

The simulation of quantum dynamics in molecular switches is investigated with the help of an ab initio based flexible model including non-adiabatic coupling and laser-molecule interaction. Here we focus on the ring opening reaction of furyl fulgide, switching the system from isomer C to isomer E. Due to the

model's flexibility it is possible to study the effect of different potential perturbations of internal and external origin.

The expansion from separated CoIns to a whole seam is incorporated. The resulting wave packet dynamics on the excited state is almost not affected and the wave packet relaxes to the ground state with the same geometry. The coupling efficiency is enhanced due to the enlarged integral over the coupling elements mainly in the first coupling event. Therefore the final product distribution is highly sensitive to the first transition passage and the subsequent branching in the ground state. Here we observe the transfer of the wave packet's momentum from the excited state to the ground state. Accordingly the first approach of the  $S_1$  wave packet towards the coupling region is the control knob for a quantitative ring opening which involves several challenges.

In addition to the limited optically accessible region, the wide difference of gradients along the reactive coordinates especially in the Franck–Condon region complicates the controllability by shaped femtosecond laser pulses. To induce a reaction path that leads to the wanted isomer the excited state wave packet must start from a position displaced from the Franck–Condon point. We were able either to accelerate the relaxation through the CoIns or to enhance the relative yield of the wanted isomer E by selective displacements along the reactive coordinate  $r$ . In ongoing work we will combine this concept with optimal control theory to optimize the overall process including IR- and UV-excitation.

Our first ab initio calculations show the existence of two excited state minima resulting in a barrier close to the Franck–Condon region. Therefore we tested the effect of different types of barriers in our model. Especially those in the vicinity of the Franck–Condon region cause strong interference effects of the wave packet. This diminishes the controllability because the first coupling step is decreased and the wave packet is widely spread. In addition to these static perturbations we investigated the molecular response to dynamical changes of the environment on different time scales. From our results one can deduce that solvent dynamics which generally occurs on the picosecond time scale will neither influence the ultrafast switching reaction nor its controllability. Otherwise dynamical changes on the femtosecond time scale, like the interaction with residual modes, can alter the reaction outcome.

In the future we will continue our quantum chemical calculations and incorporate the new ab initio data into our model PES to get a more detailed view of the switching process.

Furthermore we want to include the residual modes by treating them as a separated harmonic bath within the quantum dynamical description.

## Acknowledgements

The authors thank the Deutsche Forschungsgemeinschaft and the Fond der Chemischen Industrie for financial support and Arthur Nenov for contributions to the quantum chemical calculations. DG thanks the LMU Miiinchen for a PhD scholarship.

## References

- [1] B.L. Feringa (Ed.), *Molecular Switches*, Wiley VCH, 2001.
- [2] I. Burghardt, J.T. Hynes, *J. Phys. Chem. A* 110 (2006) 11411.
- [3] M. Abe, Y. Ohtsuki, Y. Fujimura, W. Domcke, *J. Chem. Phys.* 123 (2005) 144508.
- [4] S. Hahn, G. Stock, *J. Phys. Chem. B* 104 (2000) 1146.
- [5] S. Hahn, G. Stock, *J. Chem. Phys.* 116 (2002) 1085.
- [6] W. Humphrey, H. Lui, I. Logunov, H.-J. Werner, K. Schulten, *Biophys. J.* 75 (1998) 1689.
- [7] I.B. Ramsteiner, A. Hartschuh, H. Port, *Chem. Phys. Lett.* 343 (2001) 83.
- [8] J.M. Endtner, F. Effenberger, A. Hartschuh, H. Port, *J. Am. Chem. Soc.* 122 (2000) 3037.
- [9] S. Malkmus, F.O. Koller, B. Heinz, W.J. Schreier, T.E. Schrader, W. Zinth, C. Schulz, S. Dietrich, K. Rück-Braun, M. Braun, *Chem. Phys. Lett.* 417 (2006) 266.
- [10] M. Handschuh, M. Seibold, H. Port, H.C. Wolf, *J. Chem. Phys. A* 101 (1997) 502.
- [11] Y. Yokoyama, *Chem. Rev.* 100 (2000) 1717 (and ref. therein).
- [12] D. Geppert, L. Seyfarth, R. de Vivie-Riedle, *Appl. Phys. B* 79 (2004) 987.
- [13] D. Geppert, R. de Vivie-Riedle, *J. Photochem. Photobiol. A Chem.* 180 (2006) 282.
- [14] P. Celani, F. Bernardi, M.A. Robb, M. Olivucci, *J. Phys. Chem.* 100 (1996) 19364.
- [15] P. Celani, S. Ottani, M. Olivucci, F. Bernardi, M.A. Robb, *J. Am. Chem. Soc.* 116 (1994) 10141.
- [16] M. Garavelli, P. Celani, M. Fato, M.J. Bearpark, B.R. Smith, M. Olivucci, M.A. Robb, *J. Phys. Chem. A* 101 (1997) 2023.
- [17] A. Hofmann, R. de Vivie-Riedle, *J. Chem. Phys.* 112 (2000) 5054.
- [18] A. Hofmann, R. de Vivie-Riedle, *Chem. Phys. Lett.* 346 (2001) 299.
- [19] L. Kurtz, A. Hofmann, R. de Vivie-Riedle, *J. Chem. Phys.* 114 (2001) 6151.
- [20] M. Paterson, M. Bearpark, M. Robb, *J. Chem. Phys.* 121 (2004) 11562.
- [21] D. Yarkoni, *J. Chem. Phys.* 123 (2005) 204101.
- [22] M. Garavelli, C. Page, P. Celani, M. Olivucci, W. Fuss, W. Schmid, S. Trushin, *J. Phys. Chem. A* 105 (2001) 4458.
- [23] D. Geppert, PhD Thesis, LMU München, Fakultät für Chemie und Pharmazie, 2006.
- [24] D.J. Tannor, S.A. Rice, *J. Chem. Phys.* 83 (1985) 5013.
- [25] R.S. Judson, H. Rabitz, *Phys. Rev. Lett.* 68 (1992) 1500.
- [26] H. Rabitz, R. de Vivie-Riedle, M. Motzkus, K. Kompa, *Science* 288 (2000) 824.
- [27] W. Zhu, J. Botina, H. Rabitz, *J. Chem. Phys.* 108 (1998) 1953.
- [28] K. Sundermann, R. de Vivie-Riedle, *J. Chem. Phys.* 110 (1999) 1896.
- [29] N. Elghobashi, P. Krause, J. Manz, M. Oppel, *Phys. Chem. Chem. Phys.* 5 (2003) 4806.